Spring 2020

Optical Activation of GABA Release from D2-Medium Spiny Neurons

Nurat Affinnih
University at Albany, State University of New York

Optical Activation of GABA Release from D2-Medium Spiny Neurons

An honors thesis presented to the
Department of Biological Sciences
University at Albany, State University of New York
in partial fulfillment of the requirements
for graduation with Honors in Biology
and
graduation from The Honors College

Nurat Affinnih

Research Advisor: Annalisa Scimemi, Ph.D.
Second Reader: Damian Zuloaga, Ph.D.

May 2020

Abstract

Medium spiny neurons (MSNs) make up more than 95% of the cells in the striatum and therefore represent the main structures for specific information processing in the striatum. MSNs can be separated into two sub-populations based on the type of dopamine receptor they express and their target region. Roughly one-half of all MSNs express D1 dopamine receptors and send information to the *substantia nigra pars compacta* (SNc) and are called D1-MSNs. D1-MSNs are responsible for promoting movement execution. The other sub-population of MSNs expresses D2 dopamine receptors and for this reason, they are called D2-MSNs. D2-MSNs send information to the external capsule of the *globus pallidus* and suppress the execution of competing actions. Previously, our lab has shown that mice that lack the neuronal glutamate transporter EAAC1, hypo-functional in patients with obsessive-compulsive disorder (OCD), repeatedly performed stereotyped activities. In principle, this result could be explained by hyperactivity of D1-MSNs or by reduced D2-MSN activation. Since both populations of MSNs receive powerful GABAergic inputs from striatal neurons, we aimed to identify specific deficits in GABAergic inhibition onto D1- and D2-MSNs. By using slice electrophysiology and optogenetics, we show that D1-MSNs receive weaker GABAergic inputs in the absence of EAAC1, indicating that EAAC1 limits GABAergic inhibition onto D1-MSNs, not D2-MSNs. These findings suggest that one of the mechanisms by which EAAC1 might contribute to motor hyperactivity in OCD is by altering the coordinated recruitment of D1- and D2-MSNs.

Acknowledgments

I would like to thank Dr. Annalisa Scimemi, my research advisor, for giving me to the opportunity to work in her research lab. I have enjoyed my time in the lab and working on a project that aims to investigate the brain and its mechanisms. I would like to thank Dr. Damian Zuloaga for being the second reader for my thesis. I would also like to thank Mr. Maurice Petroccione for working with me on this project, training me in stereotaxic surgery, and performing the electrophysiology experiments, and analysis for this project. Additionally, I would like to thank all members of the Scimemi lab.

List of Figures

Table of Contents

Introduction

Obsessive-compulsive disorder (OCD) is a neuropsychiatric disorder characterized by intrusive thoughts and repetitive actions (Goodman, Grice, Lapidus, & Coffey, 2014). OCD affects 2.5-3% of the US population (Robbins, Vaghi, & Banca, 2019). The symptoms of OCD include obsessions and compulsions that are associated with checking, washing, worrying, and contaminations fears (Robbins et al., 2019). Patients with OCD have obsessive thoughts for more than 1 hour each day (Grant, 2014). These thoughts produce distress or anxiety, and the purpose of the compulsions is to relieve the discomfort caused by those intrusive thoughts (Grant, 2014).

There are multiple available treatments for OCD. A first-line treatment is cognitive behavioral therapy with exposure exercises and response prevention (Dold, Aigner, Lanzenberger, & Kasper, 2015). As a psychological treatment, cognitive behavioral therapy involves exercises that patients with OCD can perform in order to transform the way they think, their emotions, and behaviors to ultimately develop coping strategies to manage their illnesses (Courtois & Sonis, 2017). Exposure and response prevention, a form of cognitive behavioral therapy, involves exposing patients to triggers that invoke their obsessions, followed by active suppression of compulsions (Grant, Chamberlain, & Odlaug, 2014). Other treatments used include transcranial magnetic stimulation, deep brain stimulation, gamma knife surgery (a technique that is used to lesion intracranial structures in a non-invasive manner (Elaimy et al., 2010)), and psychosurgery (Brakoulias et al., 2019).

Pharmacological treatments include selective serotonin reuptake inhibitors (SSRIs), atypical antipsychotics and benzodiazepines, which act on the GABAergic system (Brakoulias et al., 2019). The use of pharmacological treatments is often plagued by poor responses to medication and adverse effects (Brakoulias et al., 2019). Of the 40-60% of patients who responds to SSRIs, there

is a 20-40% improvement of symptoms but there is only a 12% chance of full remission, and after use of these medications has ended, the rate of relapse is 90% (Grant et al., 2014). Some common side effects of these medications can include nausea, diarrhea, agitation, restlessness, drowsiness, and insomnia (Grant et al., 2014). In some rare cases, the pharmacological agent clomipramine can cause arrhythmias (Grant et al., 2014).

In the past years, there has been a growing interest in pharmacological agents targeting the glutamatergic system for the treatment of OCD (Wu, Hanna, Rosenberg, & Arnold, 2012). This is largely due to evidence of dysfunction in the cortical-striatal-thalamocortical (CSTC) circuitry in OCD (Wu et al., 2012). Hyperactivity in this circuitry has been implicated in patients with OCD (Ahmari et al., 2013). The main neurotransmitter in this circuit is glutamate (Wu et al., 2012). There is also evidence that glutamatergic transmission is dysfunctional in OCD (Brakoulias et al., 2019). The most common glutamate transporters in the central nervous system are glutamate/aspartate transporter (GLAST) and glutamate transporter-1 (GLT-1) (Holmseth et al., 2012). They prevent the buildup of glutamate in the extracellular space (Holmseth et al., 2012). EAAC1, another transporter that is involved in the uptake of glutamate (Holmseth et al., 2012), is plentiful in the striatum (Bellini et al., 2018). EAAC1 is also present in GABAergic neurons (Holmseth et al., 2012), where it plays a role in the synthesis of the neurotransmitter GABA from glutamate (Sepkuty et al., 2002).

In our lab, we study how GABAergic inhibition in the striatum is modified by the neuronal glutamate transporter EAAC1. The striatum is a basal ganglia nucleus that controls motor and cognitive functions (Boccalaro, Cristiá-Lara, Schwerdel, Fritschy, & Rubi, 2019). The principal cells in the striatum are GABAergic MSNs (Plenz & Wickens, 2017). These neurons make up about 95% of the cells in the striatum and can be classified into two separate subpopulations based

on their axonal projection targets and the type of dopamine receptor they express (Plenz & Wickens, 2017). D1-MSNs express the D1 dopamine receptor and project directly to the substantia nigra pars compacta (SNc), forming the so-called direct pathway (Plenz & Wickens, 2017). When they are activated, D1-MSNs initiate movement (Boccalaro et al., 2019). D2-MSNs express the D2 dopamine receptor and project indirectly to the SNc, making a stop in the *globus pallidus.* Therefore, the axonal projections of D2-MSNs form the indirect pathway (Plenz & Wickens, 2017). When activated, D2-MSNs control movement termination (Boccalaro et al., 2019). MSNs receive GABAergic inputs from each other and from various types of interneurons (Plenz & Wickens, 2017). The interactions between MSNs and interneurons affect how the striatum carries out its information processing functions (Plenz & Wickens, 2017). In the striatum, it has been shown that EAAC1 can promote the expression of D1 dopamine receptors (DIR) by limiting activation of metabotropic glutamate receptors (mGluRIs) (Bellini et al., 2018). It has been suggested that repeated motor behaviors are caused by decreased D1R expression which is caused by the activation of signaling cascades that are associated with mGluRIs in EAAC1 mice (Bellini et al., 2018). Furthermore, the question of how these mechanisms may influence glutamatergic and dopaminergic signaling in D1- and D2-MSNs has been brought forth (Bellini et al., 2018). With this project, we investigate how EAAC1 modulates GABAergic inhibition between MSNs in the striatum.

Genetics play a major role in OCD (Zike et al., 2017). In a genome-wide linkage scan of OCD, it was suggested that the chromosome region 9p24, which contains the gene *Slc1a1* may be involved (Zike et al., 2017). A strong association with the 3' region was determined when *Slc1a1* was analyzed (Zike et al., 2017). Some studies have implicated polymorphisms in the 3' gene region, with considerable evidence for linkage to the rs301430C allele, which is associated with

high expression of *Slc1al* (Zike et al., 2017). This gene, which encodes the neuronal glutamate transporter EAAC1, is abundantly expressed in the striatum (Bellini et al., 2018). Striatal GABAergic medium spiny neurons, which receive glutamatergic input from the cortex and send output to the thalamus, have been identified as sites where the gene *Slc1a1* can influence cortico-striatal signaling (Zike et al., 2017). It has been reported that ablation of EAAT3/EAAC1 leads to decreases in locomotion, stereotypy, and early gene induction in the dorsal striatum after administration of amphetamine (Zike et al., 2017). This ablation also leads to diminished grooming, an OCD-like behavior (Zike et al., 2017).

EAAC1 is concentrated to peri-synaptic and postsynaptic regions (Zike et al., 2017). In these regions, it has been shown to buffer glutamate concentrations around peri/extra-synaptic NMDA and metabotropic receptors, transport glutamate into the cell for GABA synthesis, and transport cysteine into the cell to synthesize glutathione and prevent oxidative stress (Zike et al., 2017). It has been suggested that glutamatergic dysfunction plays a part in OCD (Porton et al., 2013). Three *Slc1a1* isoforms have been shown to prevent glutamate uptake (Porton et al., 2013). It has also been found that people with OCD have abnormal levels of glutamate in their brains (Porton et al., 2013). Additionally, patients with OCD also have higher concentrations of glutamate in their cerebrospinal fluids (Porton et al., 2013). Some studies suggested that mice with OCD-like behaviors may have abnormal glutamatergic circuitry in their striatum (Porton et al., 2013). In our lab, mice that lack EAAC1 exhibit frequent grooming (Bellini et al., 2018). This frequent grooming, as well as a disrupted structure of episodes of grooming indicate that EAAC$^{-/-}$ mice may have functional abnormalities in their striatum (Bellini et al., 2018). The dorsal striatum is separated into the dorsomedial striatum (DMS) and the dorsolateral striatum (DLS), and both structures receive inputs from the cortex (Lipton, Gonzales, & Citri, 2019). Studies have shown

that while the DMS is linked to goal-directed actions, the DLS is involved with habitual actions (Lipton, Gonzales, & Citri, 2019). The DLS has also been associated with the performance of innate sequences, for instance, grooming, and acquired skills such as learning to balance on a moving rotarod (Lipton, Gonzales, & Citri, 2019). Furthermore, rats with lesions in the DLS have disruptions in the stereotypy of grooming sequences, indicating that the DLS is essential for the sequencing of compulsive grooming (Lipton, Gonzales, & Citri, 2019). We hypothesize that the frequent grooming behavior in our mice might be triggered by decreased GABAergic inhibition onto D1-MSNs in the DLS in the mice. What is unknown is where this inhibition is coming from. Therefore, our experiments aim at addressing this question.

Materials and Methods

Stereotaxic Surgeries – As a first step, we set up the surgical room by preparing our surgical tools and supplies. We also made sure that the anesthesia system (isoflurane) that we were using was prepared for anesthesia induction by weighing the containers of isoflurane and checking to make sure that their weights had not gone beyond 50 grams over their initial weights. We also checked that we had enough oxygen for the surgery by making sure that the oxygen tank did not have to be refilled. Next, we went to the room that housed the mice and selected the cage that contained the litter that we were performing surgeries on. These mice have either of the following genotypes: $D1_{Cre/+}$:$Ai9_{Tg/Tg}$ (or $Ai9_{Tg/0}$):$EAAC1_{-/-}$ (or $EAAC1_{+/+}$) or $A2A_{Cre/+}$:$Ai9_{Tg/Tg}$ (or $Ai9_{Tg/0}$):$EAAC1_{-/-}$ (or $EAAC1_{+/+}$). $D1_{Cre/+}$ mice express Cre recombinase under the control of D1 dopamine receptors (Bellini et al., 2018). $A2A_{Cre/+}$ mice express Cre recombinase under the control of the adenosine receptor 2. D2 dopamine receptors colocalize with this receptor (Bellini et al., 2018). Ai9 is used to report expression of Cre (Bellini et al., 2018). Through the cre-lox recombination system, we are later able to express and activate channelrhodopsin (ChR2) specifically in MSNs. Back at the surgical room, we selected one mouse to work on. We weighed the mouse and placed it in the anesthesia chamber to induce anesthesia (5% isoflurane was used for this). After 2 min, we took the mouse out of the anesthesia chamber and placed it on a paper towel. We then used a syringe to apply hair remover lotion (Nair) onto the head of the mouse. We put the mouse in the induction chamber for another two minutes for the Nair to take effect. After these 2 min, we used cotton swabs and distilled water to remove the Nair and hair from the mouse's head. We then positioned the mouse onto a heating pad in the stereotaxic frame. At this point, we set the concentration of isoflurane to 3%. We used ear bars to hold the mouse's head to keep it steady in the stereotaxic frame. We then applied lidocaine, a local analgesic, to the top of mouse's

head and waited for 2 min for it to take effect. Using cotton swabs, we cleaned the mouse's head with betadine and ethanol, three time each and alternating. We pinched the mouse's tail and toes to make sure that it was under anesthesia. If the mouse did not show any response to these pinches, we continued with the procedure, but if it did, then we increased the concentration of anesthesia and waited for one minute and repeated the pinches again. We used the scalpel to make a mid-sagittal skin incision from behind the eyes to ears (we wiped any blood on the surface of the skull and around the incision using phosphate-buffered saline [PBS]). Moving the skin of the incision around, we found bregma and selected the "Set Bregma" option on the microinjection system (Neurostar). Next, we used the microinjection system to locate the injection site in the right hemisphere of skull by using the coordinates +0.7 mm (Anterior – Posterior) and +2.2 mm (Medial – Lateral). Once the injection spot was identified, we drilled the skull at the injection spot in order to thin the skull and make it easier for the Hamilton syringe to penetrate through it. When the skull was thinned, we used the microinjection system to move the Hamilton syringe carefully and slowly into the dorsolateral striatum (DLS) by using the coordinate +3.5 mm (Dorsal – Ventral). After reaching +3.5 mm (Dorsal – Ventral), we waited for 1 min to allow the structures that we passed though on the way to the striatum to regain their shapes. We then injected 0.2 µl of the ChR2 virus (Serotype: 5 DIO-AAV: AAV-EF1a-DIOhChR2 (H134R)-EYFP-WPRE-pA) into the DLS at 0.05 µl/min and waited for 1 minute for the ChR2 to spread. We withdrew the syringe slowly and carefully to halfway out of the skull and waited for 30 s to allow the ChR2 to diffuse through the brain tissue. We then withdrew the syringe away from the skull. Next, we used the microinjection system to locate injection site in the left hemisphere of skull and repeated the same procedure. Next, we released the mouse from the stereotaxic frame and placed it on the surgical napkin. We used a plastic pipette to add a drop of PBS to the skull to moisten it and make it easier to pull the

skin on either side of the incision together. We then added surgical glue to the closed incision. We added lidocaine and antiseptic to the closed incision. We gave the mouse a 0.1 ml injection of saline in order for to regain fluids. We placed the mouse on a heating pad in a new cage and took some bedding from its original cage and added that to the new cage so that the mouse would smell like its home cage (meaning that its mother would not reject it when it was placed back into the home cage later). After the surgery was complete, we cleaned up the surgical room and returned the cages to the housing room for the mice. Here, we labeled the new cage with proper information about the mouse that surgery had been performed on and with the surgeon's contact information. We also gave the mouse some food and water. We returned the next day to check on the mouse recovery and placed it back into its home cage. The mouse brain was harvested three weeks later for electrophysiological experiments and to assess the transfection of the ChR2. ChR2 is a light-gated ion channel that can be used to neuroscience for light-induced activation of specific cells (Schneider et al., 2015). It allowed us to individually activate only D1-MSNs or only D2-MSNs in order to determine their effects on the MSNs receiving inputs (GABAergic inhibition) from them using electrophysiology.

Electrophysiology - We obtained striatal slices from C57-BL/6 mice of either sex (P24-35) that were deeply anesthetized with halothane and decapitated in accordance with SUNY Albany Animal Care and Use Committee guidelines. We rapidly removed the brain and placed it in ice-cold slicing solution bubbled with 95% O2-5% CO2, containing (in mM): 119 NaCl, 2.5 KCl, 0.5 $CaCl_2$, 1.3 $MgSO_4 \cdot H_2O$, 4 $MgCl_2$, 26.2 $NaHCO_3$, 1 NaH_2PO_4, and 22 glucose; 320 mOsm; pH 7.4. We prepared striatal slices (250 μm thick) using a vibrating blade microtome (VT1200S, Leica Microsystems, Wetzlar, Germany). After sectioning, we stored the slices in this solution in a

submersion chamber at 36°C for 30 min and at room temperature for at least 30 min and up to 4 hr. The recording solution contained (in mM): 119 NaCl, 2.5 KCl, 2.5 $CaCl_2$, 1 $MgCl_2$, 26.2 $NaHCO_3$, 1 NaH_2PO_4, 22 glucose; 300 mOsm; pH 7.4. We obtained whole-cell patch clamp recordings from MSNs that were identified under infrared-differential interference contrast using an upright fixed stage microscope (BX51 WI, Olympus Corporation, Tokyo, Japan). The internal solution that we used to record the MSNs contained (in mM): 120 KCH_3SO_3, 10 EGTA, 20 HEPES, 2 MgATP, 0.2 NaGTP, 5 QX-314Br, 5 NaCl; 290 mOsm; pH 7.2.

Data Acquisition **-** We obtained all recordings under voltage-clamp configuration using a Multiclamp 700B amplifier and a 10 KHz low-pass filter (Molecular Devices, Sunnyvale, CA). We digitized all traces at 10 KHz and analyzed them off-line with a custom-made software (A.S.) written in IgorPro 6.36 (Wavemetrics, Lake Oswego, OR). The electrode resistance was ∼5 MΩ. We monitored the series resistance throughout the experiments by applying a −5 mV pulse, 100 ms before evoking the synaptic currents. We discarded data if the series resistance changed more than 20% during the course of the experiment. We evoked transporter currents by delivering constant voltage electrical pulses (50 μs) through bipolar stainless-steel electrodes (Cat. MX21AES (JD3); Frederick Haer Company, Bowdoin, ME) placed in DLS striatum. We delivered single and paired pulses (100 ms inter-pulse interval) every 10 s. For the ChR2 experiments, we delivered a blue light stimulus every 30 s. All experiments were performed at room temperature (22–25°C).

Data Analysis **-** We analyzed all data using custom-made software written in Igor Pro (Wavemetrics, Lake Oswego, OR). Data are presented as mean ± SEM unless otherwise stated.

All experiments were performed on multiple mice of either sex. Statistical significance was determined by Student's paired or unpaired t test, as appropriate (IgorPro 6.36). Differences were considered significant at $p<0.05$ (*$p<0.05$; **$p<0.01$; ***$p< 0.001$).

Results

EAAC1 increases the quantal size of GABAergic mIPSCs in D1-MSNs – By using whole-cell patch clamp recordings in voltage clamp mode, we recorded synaptic currents and measured the amplitude of GABAergic inhibitory post-synaptic currents (IPSCs) in MSNs in acute striatal slices. In these electrophysiology experiments, we compared differences in IPSC amplitudes in DLS MSNs of wild type and EAAC1$^{-/-}$ mice. In our previous experiments, we recorded miniature IPSCs (mIPSCs) from D1- and D2-MSNs. The mIPSC amplitude was smaller in D1-MSNs of EAAC1$^{-/-}$ mice, suggesting that EAAC1 can control the quantal size of these events. TFB-TBOA (5 µM), a potent inhibitor of glutamate transporters, reduced the mIPSC amplitude in D1 and D2-MSNs. This effect was more pronounced in wild type than EAAC1$^{-/-}$ mice, suggesting a role for EAAC1 in regulating the quantal size of GABAergic mIPSCs (**Fig. 1,** A: ****p=4.3e-4,* B: **p=0.04,* C: **p=0.03,* D: ***p=3.1e-3*). These experiments also showed that the mIPSC frequency in EAAC1$^{+/+}$ D1-MSNs decreased significantly in the presence of TFB-TBOA, while the mIPSC frequency in EAAC1$^{+/+}$ D2-MSNs was not reduced significantly in the presence of TFB-TBOA. Considering EAAC1$^{-/-}$, TFB-TBOA did not significantly reduce the mIPSC frequency in D1-MSNs, but it did in D2-MSNs.

To support these findings, we repeated the TFB-TBOA application on IPSCs recorded by delivering electrical stimuli to the DLS via a bipolar stainless-steel electrode. Consistent with previous data, TFB-TBOA reduced the IPSC amplitude in D1- and D2-MSNs, in wild type and EAAC1$^{-/-}$ mice (**Fig. 1,** A: ****p=4.3e-4*, B: **p=0.04*, C: **p=0.03,* D: ***p=3.1e-3*). EAAC$^{+/+}$ D1-MSN exhibited a significantly larger decrease in amplitude of evoked IPSCs, compared to EAAC1$^{+/+}$ D2-MSNs, EAAC$^{-/-}$ D1-MSNs, and EAAC1$^{-/-}$ D2-MSNs, when TFB-TBOA was used (**Fig. 2,** **p=0.01, ***p=4.8e-3*). Since this effect was most pronounced on IPSCs recorded from

D1-MSNs, it suggests the existence of a preferential role for EAAC1 at GABAergic synapses onto D1-MSNs.

EAAC1 increases GABA release from D1- to D1-MSNs – To determine which neurons providing GABAergic innervation onto D1-MSNs are most susceptible to EAAC1, we developed an optogenetic strategy that allowed us to activate selectively D1- or D2-MSNs. To do this, we transfected the DLS of $D1_{Cre/+}$ or $A2A_{Cre/+}$ mice with a floxed viral construct encoding the light-gated ion channel ChR2.We performed stereotaxic surgery and injected ChR2 bilaterally into the DLS. After a few weeks, we prepared acute striatal slices. We activated ChR2 by delivering blue light stimuli through the epifluorescence port of an inverted microscope. The biophysical properties of these currents are shown in **Fig. 4.** We then recorded mIPSCs from these slices. The number and frequency of the mIPSCs provided data about the identity of the MSNs that we were recording from. D2-MSNs exhibited more mIPSCs than D1-MSNs. After recording the mIPSCs, the ChR2 was activated by blue light application on the slices, and the slices were imaged. The ChR2 viral construct contained a Yellow Fluorescent Protein which allowed us to determine if our slices were truly transfected with ChR2. We were able to successfully transfect the DLS with ChR2 (**Fig. 3**). Delivering blue light to the slices, led to the flow of positively charged ions across the channels in the cells that had been transfected with ChR2 (**Fig. 4A, B**). The flow of the ions across the channels lead to an inward current and then an outward current as the membrane voltage increased beyond +20 mV (**Fig. 4A, B**). When we activated ChR2 in D2-MSNs, as we increased the intensity of the blue light on our cells, the evoked responses produced by the D2-MSNs increased as well (**Fig. 4C**). In addition, D1-MSNs did not exhibit any response when the ChR2 was activated, targeting only D2-MSNs. This indicated successful cell-specific activation of D2-MSNs in the DLS. Following activation of the D2-MSNs, we performed electrical recordings from

D1-MSNs where we recorded amplitude of IPSCs received from the D2-MSNs that were activated (**Fig. 5**). There was not a significant difference between the amplitude of IPSCs recorded from EAAC1$^{+/+}$ and EAAC1$^{-/-}$ D2-MSNs inhibiting D1-MSNs (**Fig. 5**). There were similar results for EAAC1$^{+/+}$ and EAAC1$^{-/-}$ D2-MSNs inhibiting other D2-MSNs (**Fig. 5**).

Discussion

Our results indicate that EAAC1 does not play a role in the inhibition of D1-MSNs by D2-MSNs since there is not a significant difference in the amplitude of IPSCs between EAAC1$^{+/+}$ and EAAC1$^{-/-}$ D2-MSNs inhibiting D1-MSNs. Therefore, D2-MSNs cannot be the source of decreased GABAergic input onto D1-MSNs when EAAC1 is not present. Compared to other regions of the brain, EAAC1 is abundantly expressed in the striatum (Bellini et al., 2018). EAAC1 has been shown to limit the activation of metabotropic glutamate receptors (mGluRIs) in the striatum, leading to the promotion of D1 dopamine receptor expression (D1R) (Bellini et al., 2018). Activation of signaling cascades coupled to mGluRIs brings about decreased expression of D1R and generates repeated motor behaviors (Bellini et al., 2018). EAAC1 has been shown to aid in the synthesis of the neurotransmitter GABA (Sepkuty et al., 2002). When there is a lack of EAAC1, there is a reduction in glutamate transporter activity (Sepkuty et al., 2002). When EAAC1 is knocked down in rats, there is an abundance of excitability in thalamocortical slice recordings when compared with rats expressing EAAC1 (Sepkuty et al., 2002). Mice that lack EAAC1 exhibit repeated stereotyped activities, such as frequent grooming. We thought that these behaviors were caused by decreased GABAergic inhibition onto D1-MSNs. D1-MSNs receive GABAergic inputs for other MSNs and other local GABAergic interneurons in the DLS. We wanted to find out which of these sources of GABAergic inputs were causing a decrease in the GABAergic signals received by D1-MSNs. To accomplish this, we had to examine the GABAergic inhibition of different MSNs separately. We did this by using ChR2, a light-gated ion channel that can be used to neuroscience for light-induced activation of specific cells (Schneider et al., 2015). Using this channel, we were able to individually activate only D1-MSNs or only D2-MSNs in order to determine their effects on the MSNs receiving inputs from them. Our data show that EAAC1 limits GABAergic inhibition

onto D1-MSNs, not D2-MSNs. These findings suggest that one of the mechanisms by which EAAC1 might contribute to motor hyperactivity in OCD is by altering the coordinated activation of D1- and D2-MSNs. In the future, perhaps we can look at other glutamate transporters and determine whether they are compensating for the lack of EAAC1 in D2-MSNs in EAAC$^{-/-}$ mice. This may also contribute to the ultimate goal of this project, which is to find out more about GABAergic inhibition and how it relates to striatal hyperactivity in OCD. It has been found that D2-MSNs may detect dopamine differently than D1-MSNs (Yapo et al., 2017). Recently, we have started using dLight, a dopamine sensor (Cosme, Palissery, & Lerner, 2018) that will allow us to target dopamine release by MSNs in the striatum. Previously, dLight has been used in the striatum to tract learning-induced changes (Patriarchi et al., 2018). It has also been used to find changes in dopamine release in the striatum during the sleep/wake cycle, with more dopaminergic responses during wakefulness compared to during sleep (Dong et al., 2019). GABA had previously been thought to regulate dopamine, and recently, it was suggested that GABA directly inhibits the release of dopamine in the striatum (Lopes, Roberts, Siddorn, Clements, & Cragg, 2019). Perhaps considering the above stated facts and our results that EAAC1 does not limit GABAergic inhibition onto D2-MSNs can serve to provide an explanation regarding the differences in inhibition between D1-and D2-MSNs in EAAC$^{+/+}$ and EAAC1$^{-/-}$ mice in OCD. Furthermore, it may also shape and define the next steps necessary to take to better our understanding of the striatum and its functions in relation to MSNs.

Figures

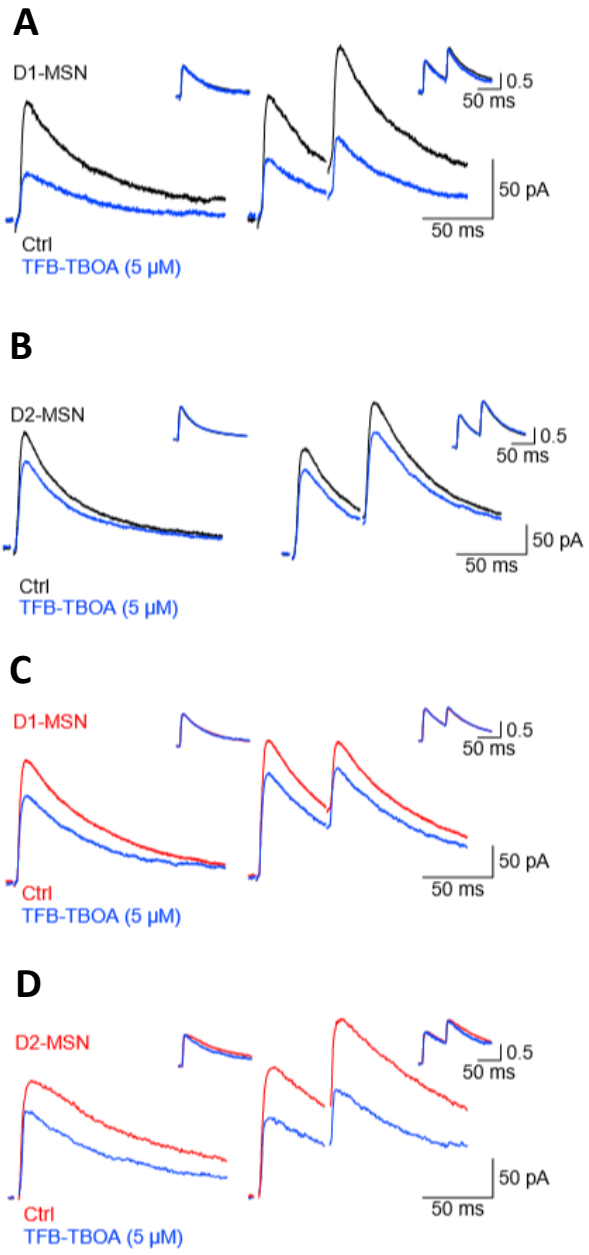

Figure 1. TFB-TBOA decreases amplitude of evoked IPSCs in EAAC1$^{+/+}$and EAAC1$^{-/-}$ D1-MSNs and EAAC1$^{+/+}$ and EAAC1$^{-/-}$ D2-MSNs. (A) The amplitude of IPSCs recorded from EAAC1$^{+/+}$ D1-MSNs is reduced in the presence of TFB-TBOA. **(B)** The amplitude of IPSCs recorded from EAAC1$^{+/+}$ D2-MSNs is reduced in the presence of TFB-TBOA. **(C)** In EAAC1$^{-/-}$ mice, the amplitude of IPSCs recorded in D1-MSNs is reduced in the presence of TFB-TBOA. **(D)** In the presence of TFB-TBOA, the amplitude of IPSCs is reduced in D2-MSNs of EAAC1$^{-/-}$ mice.

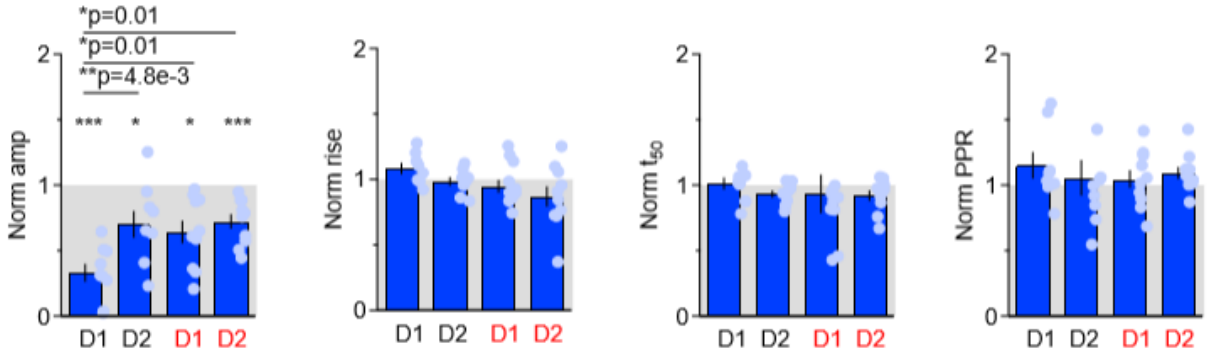

Figure 2. EAAC1$^{+/+}$ D1-MSNs have decreased amplitude of evoked IPSCs in the presence of TFB-TBOA. IPSCs were recorded in D1-MSNs and D2-MSNs. After the addition of TFB-TBOA, reduced IPSCs were recorded in D1-MSNs from EAAC1$^{+/+}$ mice, compared to other MSNs (D2-MSNs from EAAC1$^{+/+}$ mice and D1-and D2-MSNs from EAAC1$^{-/-}$ mice).

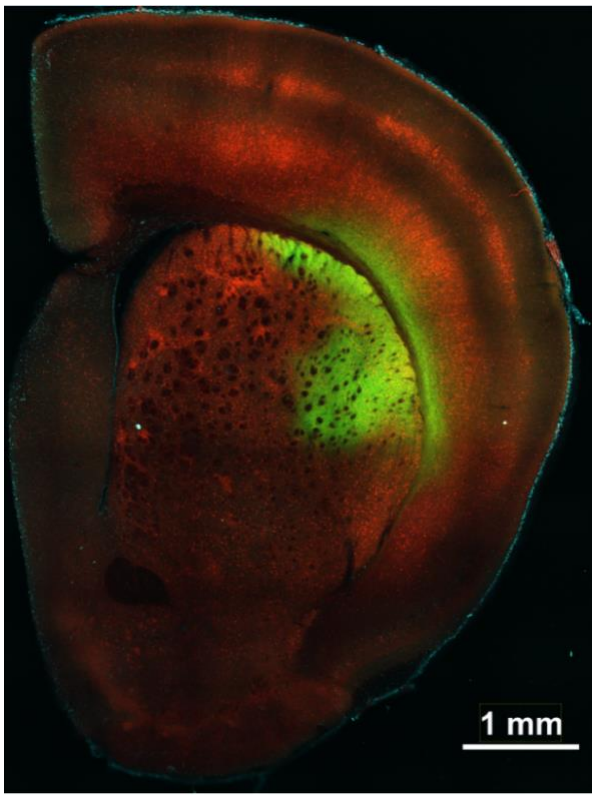

Figure 3. DLS transfected with ChR2. After stereotaxic delivery of ChR2 into the DLS, the transfected brain slices were imaged. ChR2-expressing neurons are green. Nuclear DAPI staining is shown in blue. tdTomato expressing neurons are in red.

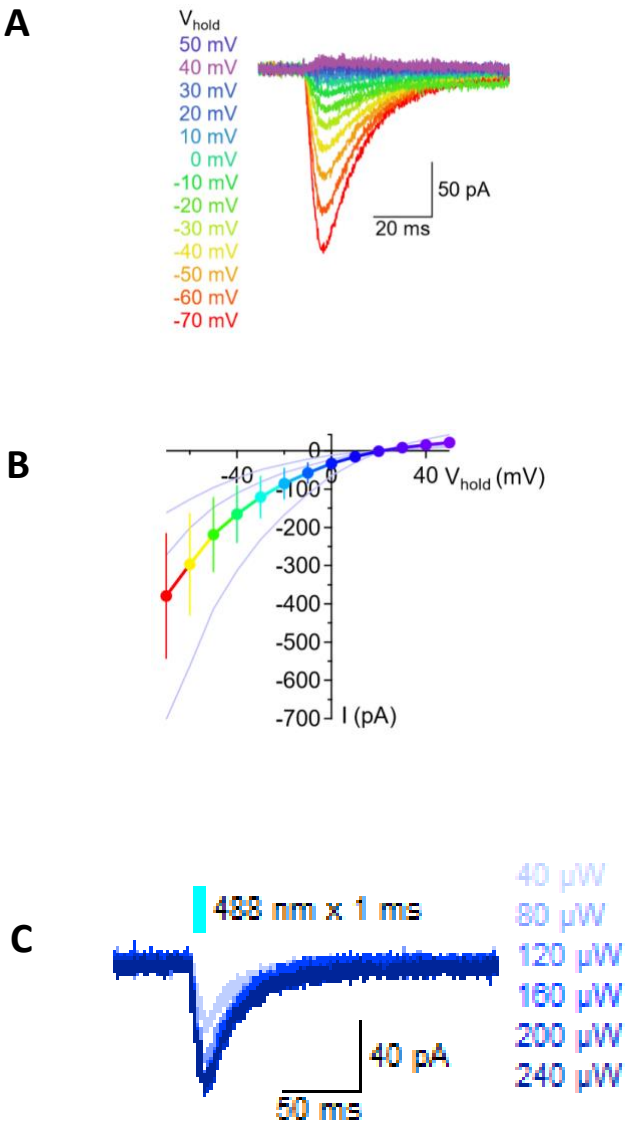

Figure 4. Biophysical properties of ChR2-transfected cells. (A) Raw tracings of current changes during ChR2 activation show an inward current between -70 mV and +50 mV. **(B)** Blue light activation of ChR2 results in an inward current between -60 mV and +20 mV. After +20 mV, there is an outward current. **(C)** After ChR2 transfection, blue light was delivered onto the brain slices during electrophysiology experiments in order to activate D2-MSNs. Increasing the intensity of blue light (470 nm) on striatal slices transfected with ChR2 increases responses exhibited by D2-MSNs in the DLS.

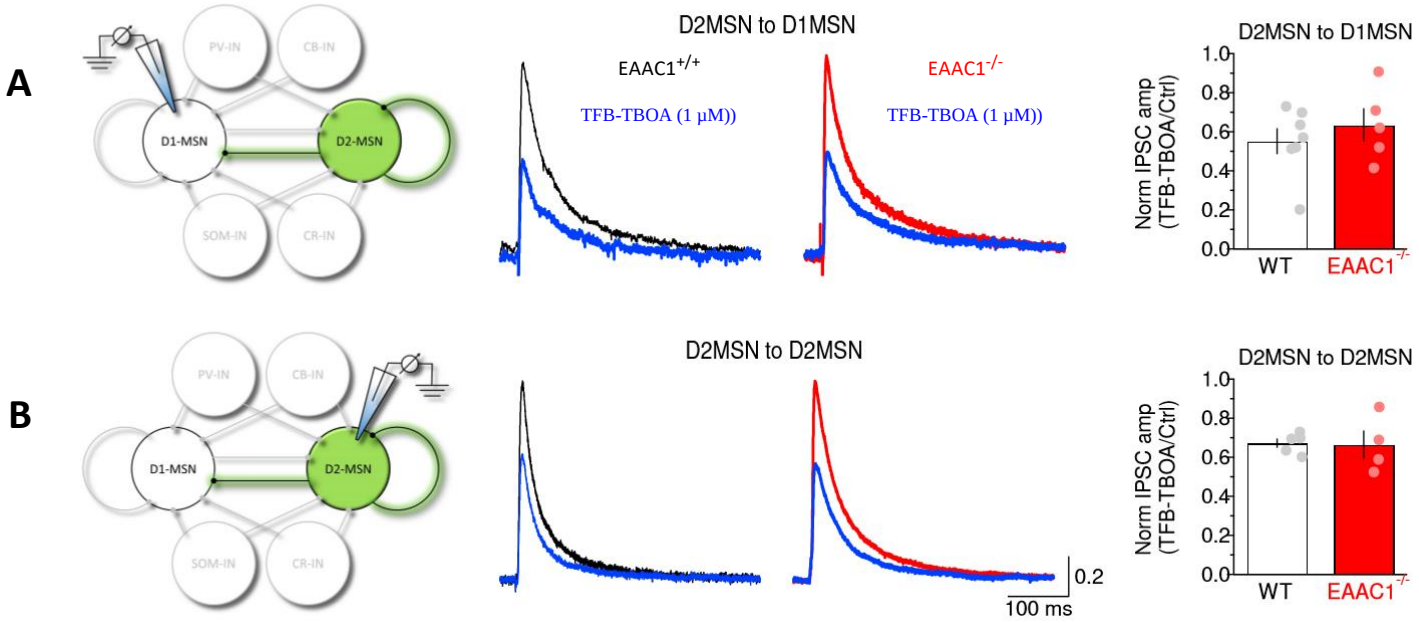

Figure 5. EAAC1 does not contribute to inhibition from D2-MSNs onto D1-MSNs. EAAC1$_{+/+}$ and EAAC1$_{-/-}$ D2-MSNs transfected with ChR2 were activated with blue light and electrical recordings were performed from D1-MSNs and D2-MSNs in order to measure amplitude of IPSCs. **(A)** There was no significant difference in normalized IPSC amplitude between EAAC1$_{+/+}$ and EAAC1$_{-/-}$ when activating D2-MSNs and recording from D1-MSNs. **(B)** There was no significant difference in normalized IPSC amplitude between EAAC1$_{+/+}$ and EAAC1$_{-/-}$ when activating D2-MSNs and recording from D2-MSNs.

References

Ahmari, S. E., Spellman, T., Douglass, N. L., Kheirbek, M. A., Simpson, H. B., Deisseroth, K., Gordon, J. A., & Hen, R. (2013). Repeated cortico-striatal stimulation generates persistent OCD-like behavior. *Science* (New York, N.Y.), *340*(6137), 1234–1239.

Bellini, S., Fleming, K. E., De, M., McCauley, J. P., Petroccione, M. A., D'Brant, L. Y., Tkachenko, A., Kwon, S., Jones, L. A., & Scimemi, A. (2018). Neuronal glutamate transporters control dopaminergic signaling and compulsive behaviors. *The Journal of Neuroscience: The Official Journal of the Society for Neuroscience*, *38*(4), 937–961.

Boccalaro, I. L., Cristiá-Lara, L., Schwerdel, C., Fritschy, J., & Rubi, L. (2019). Cell type-specific distribution of GABAA receptor subtypes in the mouse dorsal striatum. *The Journal of Comparative Neurology*, *527*(12), 2030-2046.

Brakoulias, V., Starcevic, V., Albert, U., Arumugham, S. S., Bailey, B. E., Belloch, A., Borda, T., Dell'Osso, L., Elias, J. A., Falkenstein, M. J., Ferrao, Y. A., Fontenelle, L. F., Jelinek, L., Kalogeraki, L., Kay, B., Laurito, L. D., Lochner, C., Maina, G., Marazzitt, D., Martin, A., Matsunaga, H., Miguel, E. C., Morgado, P., Mourikis, I., Pasquini, M., Prerez Rivera, R., Sriramya, P., Reddy, J. Y. C., Riemann, B. C., Conceição do Rosario, M., Shavitt, R. G., Stein, D. J., Viswasam, K., Wang, Z., Fineberg, N. A. (2019). Treatments used for obsessive–compulsive disorder—An international perspective. *Human Psychopharmacology*, *34*(1), e2686.

Cosme, C. V., Palissery, G. K., & Lerner, T. N. (2018). A dLight-ful new view of neuromodulation. *Trends in Neurosciences*, *41*(9), 566–568.

Courtois, C. A., & Sonis, J. (2017). Guideline: What is cognitive behavioral therapy? *American Psychological Association*, 1-119.

Dold, M., Aigner, M., Lanzenberger, R., & Kasper, S. (2015). Antipsychotic augmentation of serotonin reuptake inhibitors in treatment-resistant obsessive-compulsive disorder: An update meta-analysis of double-blind, randomized, placebo-controlled trials. *The International Journal of Neuropsychopharmacology*, *18*(9), pyv047.

Dong, H., Wang, J., Yang, Y. F., Shen, Y., Qu, W. M., & Huang, Z. L. (2019). Dorsal striatum dopamine levels fluctuate across the sleep-wake cycle and respond to salient stimuli in mice. *Frontiers in Neuroscience*, *13*, 242.

Elaimy, A. L., Arthurs, B. J., Lamoreaux, W. T., Demakas, J. J., Mackay, A. R., Fairbanks, R. K., Greeley, D. R., Cooke, B. S., & Lee, C. M. (2010). Gamma knife radiosurgery for movement disorders: a concise review of the literature. *World Journal of Surgical Oncology*, *8*, 61.

Goodman, W. K., Grice, D. E., Lapidus, K. A., & Coffey, B. J. (2014). Obsessive-compulsive disorder. *The Psychiatric Clinics of North America*, *37*(3), 257–267.

Grant, J. E., Chamberlain, S. R., & Odlaug, B. L. (2014). *Clinical guide to obsessive compulsive and related disorders*. New York, NY: Oxford University Press.

Grant, J. E. (2014). Clinical practice: obsessive-compulsive disorder. *New England Journal of Medicine, 371*(7), 646–653.

Lopes, E. F., Roberts, B. M., Siddorn, R. E., Clements, M. A., & Cragg, S. J. (2019). Inhibition of nigrostriatal dopamine release by striatal $GABA_A$ and $GABA_B$ receptors. *The Journal of Neuroscience: The Official Journal of the Society for Neuroscience, 39*(6), 1058–1065.

Patriarchi, T., Cho, J. R., Merten, K., Howe, M. W., Marley, A., Xiong, W. H., Folk, R. W., Broussard, G. J., Liang, R., Jang, M. J., Zhong, H., Dombeck, D., von Zastrow, M., Nimmerjahn, A., Gradinaru, V., Williams, J. T., & Tian, L. (2018). Ultrafast neuronal imaging of dopamine dynamics with designed genetically encoded sensors. *Science* (New York, N.Y.), *360*(6396), eaat4422.

Plenz, D., & Wickens, J. R. (2017). The striatal skeleton: Medium spiny projection neurons and their lateral connections. In H. Steiner & K. Tseng (Eds.), *Handbook of basal ganglia structure and function* (pp. 121-132). Chicago, IL: Elsevier/Academic Press.

Porton, B., Greenberg, B. D., Askland, K., Serra, L. M., Gesmonde, J., Rudnick, G., Rasmussen, S. A., & Kao, H. T. (2013). Isoforms of the neuronal glutamate transporter gene, SLC1A1/EAAC1, negatively modulate glutamate uptake: Relevance to obsessive-compulsive disorder. *Translational Psychiatry, 3*(5), e259.

Robbins, T. W., Vaghi, M. M., & Banca, P. (2019). Obsessive-compulsive disorder: Puzzles and prospects. *Neuron, 102*(1), 27–47.

Schneider, F., Grimm, C., & Hegemann, P. (2015). Biophysics of channelrhodopsin. *Annual Review of Biophysics, 44*(1), 167–186.

Sepkuty, J. P., Cohen, A. S., Eccles, C., Rafiq, A., Behar, K., Ganel, R., Coulter, D. A., & Rothstein, J. D. (2002). A neuronal glutamate transporter contributes to neurotransmitter GABA synthesis and epilepsy. *The Journal of Neuroscience: The Official Journal of the Society for Neuroscience, 22*(15), 6372–6379.

Wu, K., Hanna, G. L., Rosenberg, D. R., & Arnold, P. D. (2012). The role of glutamate signaling in the pathogenesis and treatment of obsessive-compulsive disorder. *Pharmacology, Biochemistry, and Behavior, 100*(4), 726–735.

Yapo, C., Nair, A.G., Clement, L., Castro, L.R., Hellgren Kotaleski, J. & Vincent, P. (2017), Detection of phasic dopamine by D1 and D2 striatal medium spiny neurons. *The Journal of Physiology, 595*, 7451-7475.

Zike, I. D., Chohan, M. O., Kopelman, J. M., Krasnow, E. N., Flicker, D., Nautiyal, K. M., Bubser, M., Kellendonk, C., Jones, C. K., Stanwood, G., Tanaka, K. F., Moore, H., Ahmari, S. E., & Veenstra-VanderWeele, J. (2017). OCD candidate gene SLC1A1/EAAT3 impacts basal

ganglia-mediated activity and stereotypic behavior. *Proceedings of the National Academy of Sciences of the United States of America, 114*(22), 5719–5724.